Green Chemistry

Accepted Manuscript

ROYAL SOCIETY OF CHEMISTRY

www.rsc.org/greenchem

Mechanical milling as an ecological and economical alternative to achieve homogeneous dispersion of nano-fillers into sustainable polymers.

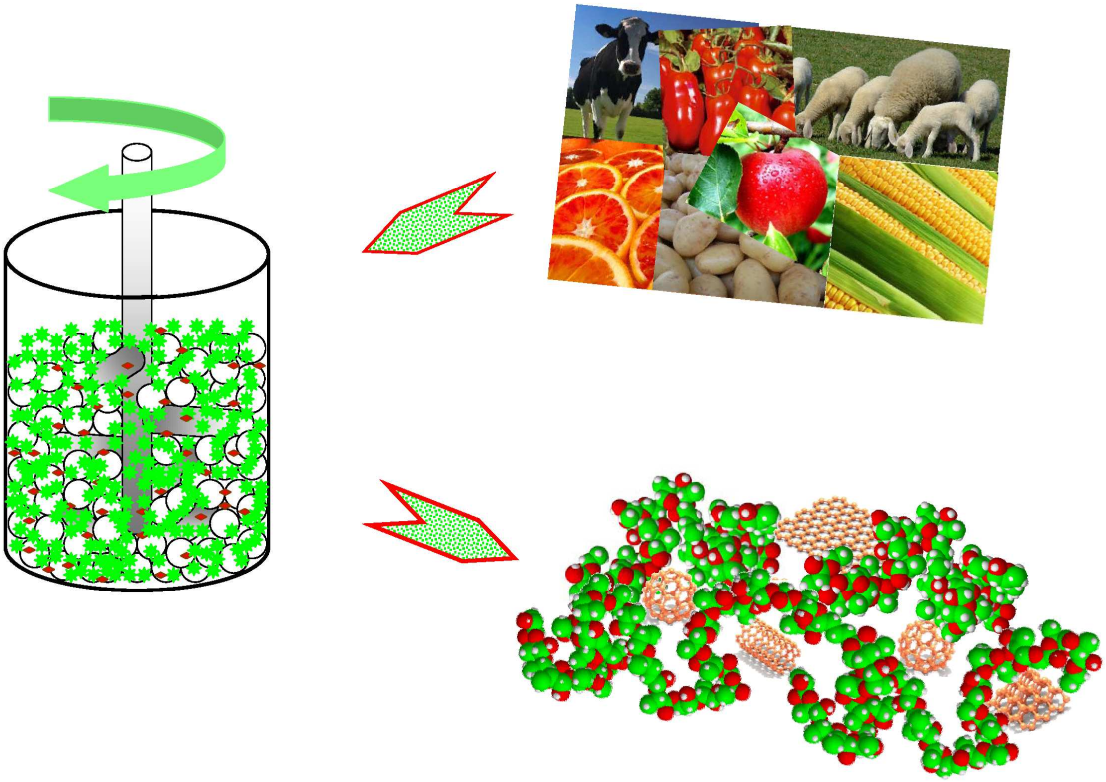

Mechanical Milling as a technology to produce structural and functional bio-nanocomposites

Giuliana Gorrasi[1*] **and Andrea Sorrentino**[2]

[1]*Department of Industrial Engineering-University of Salerno- via Giovanni Paolo II, 132, 84084 Fisciano (Salerno), Italy*
[2]*CNR, Institute for Polymers, Composite and Biomaterials (IPCB), Piazzale Enrico Fermi 1, I-80055 Portici (Napoli), Italy*
**e-mail:* ggorrasi@unisa.it

Abstract

The “solid state mixing”, such as mechanical milling (MM), represents an ecological and economical alternative to achieve homogeneous dispersion of nano-fillers into biodegradable polymers. The advantage of working at low temperature, without solvent and with almost any type of polymer matrix, opens new and unexplored routes for the preparation of advanced functional materials. The use of mechanical milling contains within itself several advantages, including a strongly reduction of the environmental disposal, the control of the degradation processes associated to the high temperature, the compatibilization of immiscible blends and the treatment of waste disposal and recycled materials. The simultaneous formation and dispersion of nanoparticles, the promotion of mechano-chemical reactions and the proper manipulation of thermo-sensitive active molecules such as antimicrobials, oxygen scavengers and antibiotics are other advantages of this process. The aim of the current work is to review the recent literature on the use of MM as green technique to produce bio-nanocomposites. It will be demonstrated how this technology could be considered an interesting option for the fabrication of novel nanostructured materials from environmental friendly resources.

1. Introduction

The homogeneous dispersion of nanoparticles into polymer matrices has attracted considerable research interest in the past few years [1–3]. Only with an effective filler distribution, it is possible to take advantage of the enormous aspect ratio of these particles to obtain composites with unique properties [4–7]. Unfortunately, the results achievable are generally limited by the re-aggregation of the nanoparticles, which determines the size distribution and the adhesion of the nanoparticles to the polymer matrix. Other limitations are related to the temperature and mechanical stress that must be applied to the polymer matrix during the dispersion process [8]. Two approaches are generally utilized for stabilize the nanoparticles against their natural tendency to aggregation [9]. Both of them require the formation of a polymer coating around the bare particles in order to increase the compatibility with the polymer matrix and to make it easier to disperse [10]. In the first approach, also known as *ex situ* approach [11], the polymer shell is obtained by dispersing the preformed inorganic particles in a polymer solution or melt by mechanical mixing, such as sonication and melt mixing. Alternatively, the shell formation can be realized by polymerization of the desired monomer with the organophilic nanoparticles dispersed in it. This approach is the most general one because there are no limitations on the kinds of nanoparticles and polymers that can be used. In the *in situ* approach, nanoparticles are generated inside the polymer matrix by appropriate thermal or chemical treatments of the precursors [12,13]. Even if with this approach it is possible to achieve very homogeneous and stable nanoparticle dispersions, this method is generally an expensive and complex solution. Therefore, it is necessary to find out new methods to achieve homogeneous dispersions, with higher ecological and economical sustainability. The solid state mixing, such as high energy mechanical milling, might be an interesting green and solvent free alternative. It has been used to produce novel polymer nanocomposites, and can be attractive also from an economical point of view [14,15]. Mechanical milling (MM) is essentially a mixing carried out by means of repeated high intensity plastic deformation. These deformations can generate composites with characteristic length scale of morphology up to the atomic scale dimensions [16]. In this way it is possible to produce a variety of non-equilibrium structures depending on the chemical properties of the processed materials [17]. The reduction of the particle size and blending of particles in new phases is the main objective of such technique. It relies on several variations and is referred by various terms: mechanical alloying (MA), high energy milling, reactive milling (RM), and mechanical activation [18]. Some investigators often used the terms mechano-chemical processing (MCP), mechano-chemical synthesis, or mechano-synthesis which refers to the mixing process in which chemical reactions and phase transformations take place for the application of mechanical energy [19,20]. The destruction of long-range order to produce an amorphous phase has been referred to as mechanical disordering (MD) [19]. Several works report the evaluation of the applicability of this technique in improving the dispersion of various fillers [21,22], enhancing the polymer properties [23,24], modifying their morphology [25], enhancing the compatibility in polymer blends [26–28], and conducting grafting reactions [21,29]. Milling process may also be employed for direct solid-state mixing of nanofiller with polymer prior to melt compounding [30]. Examples of direct modification/formation of inorganic nanostructures by means of mechanical milling are also documented [31,32].

This review provides a brief introduction to the mechanical milling, a discussion of its mechanisms and capability, the various applications proposed for polymeric bio-nanocomposites. In particular, will be analyzed the preparation and the physical properties of polymeric biodegradable matrices from natural or renewable sources filled with structural and functional nanometric fillers.

2. Milling Equipments

Different types of milling equipment are available for particle size reduction, mixing or blending, particle shape changes and production [33]. They differ in capacity, efficiency of milling and additional arrangements for heat transfer. The kinetic energy of the drive is transmitted to the grinding media and the material to be ground, the mills can be divided into two main groups: indirect and direct milling equipments. In the direct milling equipments, the kinetic energy is transmitted directly to the ground particles by means of mechanical shaft or rollers (fig. 1). Examples are the attritor, the pan, and the roll mill.

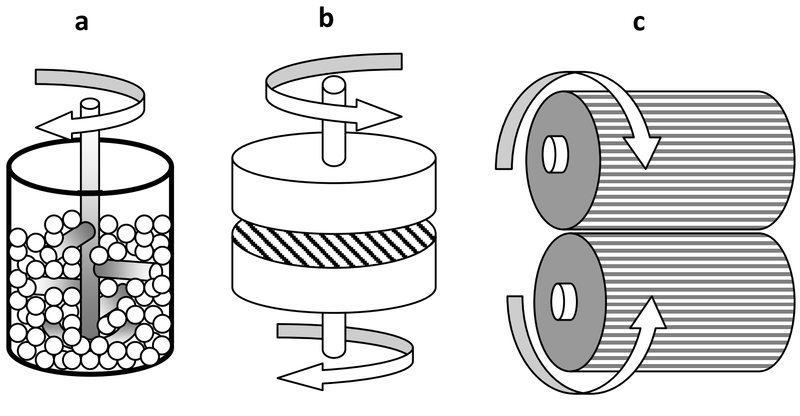

Figure 1: Schematic representation of the direct milling equipment. (a) attritor mill, (b) pan mill, (c) roll mill.

An attritor mill consists of a vertical stationary tank filled with the powder to be milled and the grinding media (fig. 1a). The mixture is then shaken by a vertical shaft with horizontal arms (impellers) rotating at a high speed. The motion causes a differential movement between the balls and the powder, providing both shearing and impact forces on the material. The final products achieved by attritors are generally spherical in shape compared to other impact-type milling equipment. The attritors are also versatile to operate under a broad range of conditions (i.e. the size and amount of grinding media, milling speed and temperature) according to the particular requirements. The Pan Mill consists of a pair of pans, i.e. a moving pan and a stationary pan, which have a similar structure (fig. 1b). The round pan is divided into equal sectors by several diametrical lines. On each sector, there are several levels, and the ridges of the levels are parallel with the dividing lines. The pair of pans is placed together, face to face, and the ridges and levels on both pans form many unit cells. The shape and volume of these unit cells change with the running of the moving pan on the stationary pan, resulting in size reduction of the materials in between. The materials suffer from strong pressure and shear forces owing to the space changes of the unit cell and move in a complex manner in both circular and radial directions, repeatedly squeezed and split from the entrance to the exit of the mill pan [34]. A roll mill consists of two horizontal steel rolls that have the same diameter and length (fig. 1c). It uses the shear force created by opposite direction of the rolls in order to crush or grind, mix, refine, disperse or homogenize materials fed inside. The materials fed between the rolls experiences very high shear stress due to the narrowing space and the different rotation speeds between the two rolls. The gaps between the rolls can be mechanically or hydraulically adjusted and maintained. Typically, the gap distance is far greater than the particle size. In some operations, the gap distance may be gradually decreased to achieve the desired level of dispersion. Both rolls are usually capable of being heated and, in some cases, the rolls may also be cooled when required. In the indirect milling equipments, the kinetic energy is transmitted to the mill body, and then it is transferred to the grinding medium and charge by friction. In that case the charge is subjected to centrifugal and gravitational forces (fig. 2). The typical mill configurations of this group are the ball mill such as tumbler ball mills, vibratory mills, and planetary mills [35].

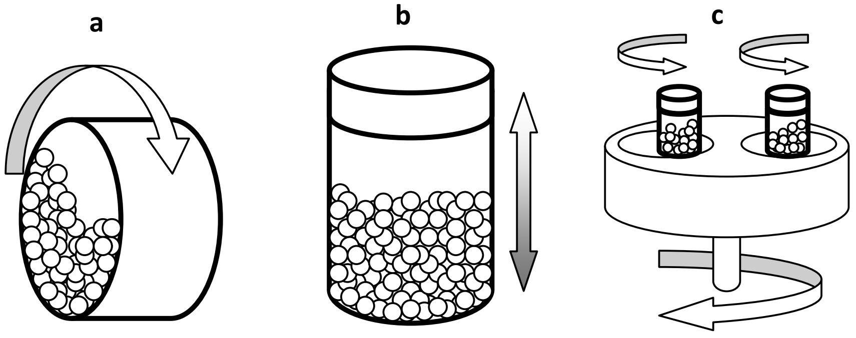

Figure 2: Schematic representation of the indirect milling equipments. (a) tumbler ball mill, (b) Vibratory (or Shaker) mill, (c) planetary ball mill.

A conventional tumbler ball mill (fig. 2a) consists of a rotating horizontal vessel partially filled with steel balls. The vessel, whose length exceeds its diameter, is fitted with shafts and rotated about its longitudinal axis. As the vessel rotates, the balls drop on the powder that is being ground. By increasing the diameter of the mill, the efficiency of operation increases. This is caused by the greater height of fall and impact energy imparted to the grinding media. The rate of grinding increases with the speed of rotation. At high speeds, however, the centrifugal force acting on the steel balls exceeds the force of gravity, and the balls are pinned to the wall of the vessel. Vibratory (or Shaker) mills (fig. 2b) are commonly used for laboratory investigations and for screening purposes. The vial containing the sample and the grinding media is secured in the clamp and it is swung energetically back and forth several thousands times a minute. The impact forces acting on the powders are function of the rate of milling, amplitude of vibration, and mass of the milling medium. High vibrational frequencies and small amplitudes of vibration allow to obtain highly milling forces compared to the attrition and vibratory mills. The most recent design of this mill incorporates forced cooling to allow prolong milling times. In cryogenic version, the vial is sealed under argon and is placed in a sleeve that allows peripheral circulation of liquid nitrogen [36]. The planetary ball mill owes its name to the typical orbital revolution movement of its vials. These are arranged on a rotating support disk, and a special drive mechanism causes them to rotate around their own axes (fig. 2c). The complex centrifugal force produced by the orbital rotation causes a continuous alternating freely movement of the grinding medium between two consecutive collisions with the walls chamber. This causes a large decrease of the friction stress during the milling. The biggest the space in the vial available for the charge materials, the longest the travelling distance of the charge materials, and the longer the distance the higher the kinetic energy that could be gain by the moving charge materials. This kinetic energy determines the amount of impact energy generated during collision. Several theoretical models have been proposed in order to evaluate the power transferred to the load during a milling process [37–39]. The basic assumption is that the mechanical energy is not continuously supplied to the charge, but it is intermittently delivered through periodic and impulsive actions. The power involved in the milling process is given by the product of the kinetic energy released in a single collision event (ΔE) and the total number of events per unit of time (N) (equation 1):

$$P = \varepsilon \cdot \Delta E \cdot N \tag{1}$$

where ε is a coefficient equal to 0 for perfect elastic collisions (no energy transfer) or equal to 1 for perfect inelastic collisions. The kinetic energy involved in the collision is then given by

$\Delta E = \frac{1}{2} m_b \cdot v_b^2$, m_b and v_b being the average mass and the velocity of the single impact event. Accordingly, specific energy (W_s) supplied to mill charge is given by equation 2 [40]:

$$W_s = \frac{1}{M}\frac{dP}{dt} = \frac{\varepsilon \cdot m_b \cdot N \cdot v_b}{M} \cdot \frac{dv_b}{dt} \qquad (2)$$

where M is the mass of the material to be ground. By assuming that the energy can only be dissipated during the impacts between the grinding media, W_s will only depend on some intrinsic parameters of the mill, such as the number and mass of the grinding materials, the rotation frequency of the vials, the grinding-to-powder weight ratio and the milling time. Although the simplicity of this approach, the equation 1 and 2 represent a very simple tools for a rough evaluation of the energy transfer, theoretically for all type of mills. According to the W_s equation, the mill equipments classified with respect to the energy provide the following classification: planetary > vibrational > attritor > tumbling mill. A more precise evaluation of W_s requires a detailed modeling approach to mill dynamics [37,41–43]. Interestingly, it has been found a good agreement between predictions and experimental observations [44,45]. The specific mill power and the specific energy transferred to the solid particles will depend on the type of mill, as well as the grinding medium of milling. For a tumbler mill, the specific mill power is 30-50 W/Kg [46]; for a vibratory mill it is 250-4500 W/Kg; for an attrition mill it is 900-14000 W/Kg and for the planetary mill it is 9000-36000 W/Kg [47]. However, it has been estimated that only about 5-15% of the specific mill power can be transferred to the polymer mixture because a large part will be dissipated as heat [47,48].

In recent years, many new and modified milling techniques have been developed and investigated. They make use the assistance of other treatments, such as ultrasonic [49], magnetic-field [50], plasma sintering [51], and microwaves [52]. The coupling effects of these treatments with the mechanical milling have proven to improve dynamically and mechanically the process, causing better stirring, crushing, and surface peeling. The activation energy was strongly reduced, leading to accelerated chemical reactions and activated nanoparticles formation. In the following are reported some example of milling process application to the preparation of several bio-nanocomposites systems.

3. Process Variables

Several parameters influence the milling process, the most important are: the type of mill, the amount of powder into the milling chamber, the size and number of the grinding medium, the milling speed, the dry or wet conditions, the temperature and the duration of the process [53].

Probably, among these, the milling time is the most important. Substantial reduction in particle size usually occurs with milling time and typically takes the form of exponential decay [18,54]. However, the level of contamination will increase with milling time and some undesirable phases may form if a powder is milled for too long times. The milling equipment is also important for the type of processing requested. It has a strong effect on the stress mechanism applied, and thus on the particle size reduction and on the product size distribution. The material used for the milling media (milling chamber, vial, balls) is important due to impact of the milling balls on the inner walls of the milling chamber [18]. Commonly, materials include various steels (stainless, tool, hardened chromium, tempered, bearing steel and tungsten carbide lined), tungsten carbide, zirconia, agate, alumina and silicon nitride. Since mass and velocity of the grinding medium is strictly related to their kinetic energy, dense materials like steel or tungsten carbide are much preferable to other materials (like ceramics). In addition, size and number should be optimized for a given mill [55]. Generally a high dense packing of grinding medium reduces the mean free path of the ball motion, while a too dilute distribution allow to minimize the collision frequency [56]. The highest collision energy can be obtained if a combination of smaller and larger balls are used to “randomize” the motion of the balls [18]. The ball to powder ratio or charge ratio is another milling parameter and represents the weight ratio of the milling balls to the powder charge. It is necessary enough space for the balls and the powder particles to move around freely in the milling chamber. Generally about 50% of the space is left empty but in attritors this value is 20-30% [18]. The control of the milling atmosphere has a huge importance, since lack of it can lead to some undesired mechano-chemical reactions or contamination in the obtained materials [16]. For this reason, generallu the milling process is carried out under vacuum or in an inert atmosphere, in presence of argon or helium [18]. Different types of liquid surfactants are also utilized to avoid powder aggregation during the milling. However, such liquids can also be an important source of contamination [17]. The temperature at which the processing takes place influences the diffusivity and defect concentration in the powder, being crucial in the phase transformations induced by milling. The temperature during milling can depend on the kinetic energy of the ball, the material characteristics and milling media [57]. On the other hand, during the milling process the material is subjected to different temperature levels. During the collisions the milled material is subjected to the local (microscopic) temperature pulses, whereas the material that moves free in the milling chamber can be considered at the overall (macroscopic) temperature [18]. The results of measurements and calculations of the macroscopic milling temperatures show that it is not so sensitive to the mill design [58]. On the contrary, the microscopic temperature can be very high, often exceeding the melting points of some of the powder component. For example, model calculations predicted an additional temperature increase of 50-

300°C for the powder compressed between the colliding milling tools in a common planetary mill [59,60]. Work by Kwon et al. [61] demonstrated that the ball diameter, as well as the presence of powder coating on the grinding balls and the vial wall during milling, has a significant influence on the ball temperature during mechanical alloying. It is suggested that the higher ball temperatures result from more oblique collisions and friction, while the lower temperature but higher intensity of the mixer mill with flat-ended vial is due to the larger portion of frontal impacts. Many high-energy mill processing are carried out in presence of cooling medium such as water, forced air-cooling or liquid nitrogen (cryo-milling) [62]. Longer milling runs are often divided into shorter periods separated by cooling breaks to avoid excessive heating [63].

4. Fracture, Dispersion and Agglomeration

The milling action produces a variety of stresses in the particles being ground; the most common are compression, attritions, shear and impact. Figure 3 shows the collision act, during which particles are firstly trapped (compressed) between two colliding media within a space occupied by a dense cloud, dispersion, or mass of powder particles [18]. The trapped volume consists of particles within the region AOB and embraces a number of particles ranging from one to several thousand. Its number is dependent on the particle size, the density and the diameter of the balls used, and the amount of powder particles used. Outside this region, the density of the powder particles decreases to the density of the loose powder in the mill. Successively, if the impacting force is sufficient, the trapped particles are compacted to form irregularly shaped macro-particles through the rearrangement and the restacking of the original particles (fig. 3). Depending on the ductility of the materials and the milling environment, agglomeration of particles may occur by welding, mechanical interlocking of spongy or rough surfaces, or molecular interaction characterized by Van der Waals forces [64,65]. As the colliding media are decelerated during the impact, a radial displacement of powder particles occurs (shear and attritions stresses). The resistance to the displacement is due to the friction between the particles and the colliding surfaces [66]. Such displacement is dependent on the surface roughness of both the particle and tools, and the degree of binding or cold welding between the agglomerated particles and mill bail surfaces. The probability of impact directly depends on the probability of a particle being captured in the grinding zone and thus depends on the particle agglomeration, fluidity, and particle transport in the mill. To enhance the milling efficiency, different grinding media shapes have been tried: cypebs, cubes, ballpebs, cylinders, etc. However, spheres are the favored shape for presenting a higher grinding surface area and reducing wear and deformation [66].

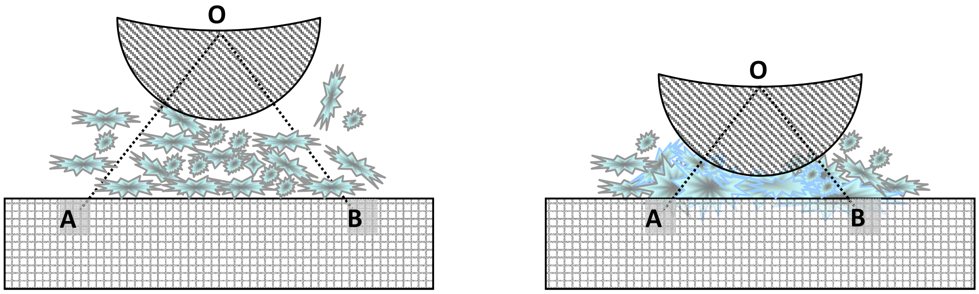

Figure 3: Model of impact event at a time of maximum impacting force.

The morphology achievable with this process depends mainly on the mechanical behavior (ductility or brittleness) of the milled powders. Very different microstructures are expected when the precursor powders are ductile, brittle or a combination of ductile-brittle materials [67]. Brittle powder systems when exposed to high level of impact force are subjected to continuous fracture. Previous cracks, defects, and inclusions in particles facilitate fracturing [68]. The microstructure of these composites changes with milling time, with a drastic reduction in size during the first milling times, up to the a particle size limit [68,69]. This limit is due to both, the plastic deformation behavior and the increased surface force cohesion between the fine particles. In figure 4, are illustrated the three basic mechanisms considered for the description of the particles fracture:

Particle abrasion: it occurs when local low intensity stresses are applied. The result is fine particles taken from the surface of the mother particle (fig. 4a).

Cleavage of particles: it occurs when slow and relatively intense compressions stresses are applied. Medium size fragments with close size distribution are produces (fig. 4b).

Fragmentation: it is a result of rapid applications of intense impact stresses. The result is the formation of small sizes fragments with a relatively wide size distribution (fig. 4c).

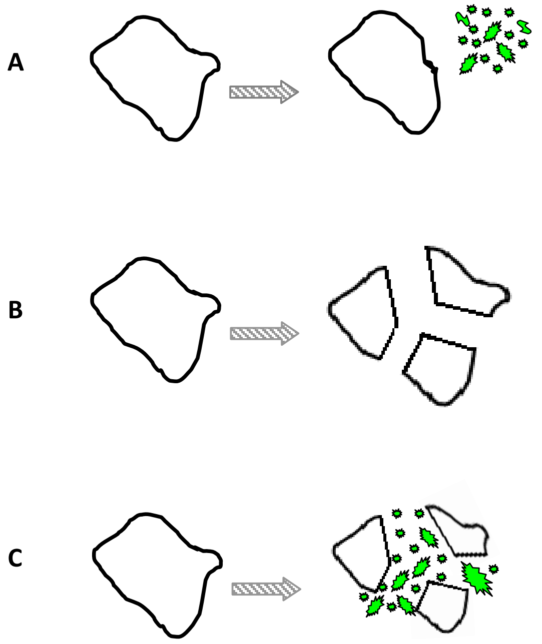

Figure 4: Basic mechanisms considered for the description of the particles fracture. A) Abrasion; B) Cleavage; C) Fracture.

In practice, the three different mechanisms never occur alone and the process of particle size reduction involves all of them with possible predominance depending on the type of the mill, the operating conditions and the type of the material being ground [67]. The morphology achievable with ductile components can be interpreted in terms of a competition between cold-welding and fracture [18]. In that case, the particles subjected to the mechanical stress, firstly, become elongated with a progressive reduction in thickness (fig. 5a). As the particles become deformed, they are subjected to fatigue failure and fragmentation. Fragments generated may combine to form agglomerates with a sandwich microstructure. A strong cold-welding between these micro layers with a further decrease in the thickness dimensions is expected. The process continues with alternate elongation and fracture of the particles. When a mixture of ductile materials is utilized, a mechanical alloy takes place, eventually aided by the heating produced by milling process [39]. In that case, with milling time, the microstructure becomes more and more refined up to the complete homogenization of the components [70,71].

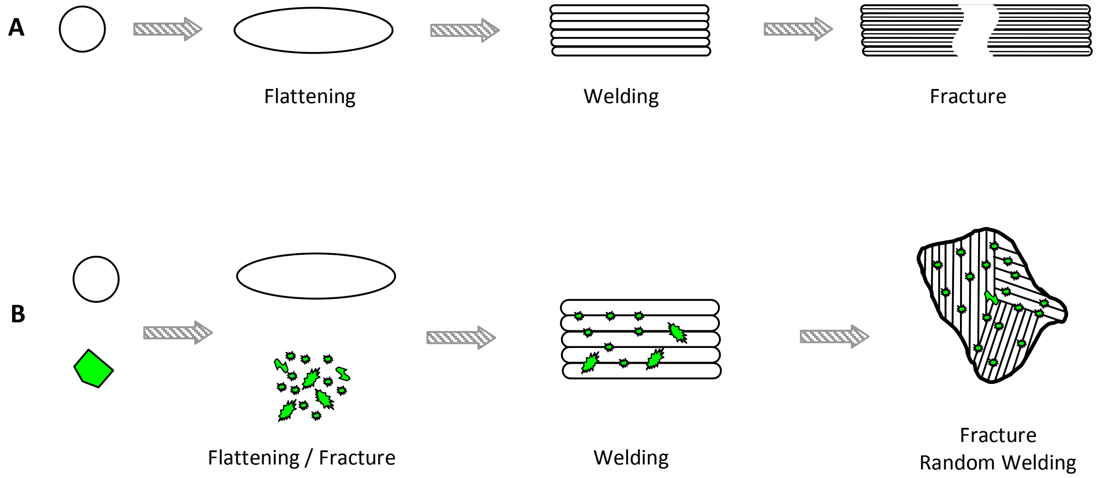

Figure 5: Schematic representation of the various stage of the mechanical alloying of: a) ductile, b) ductile-brittle system.

The evolution of microstructure during mechanical milling of ductile-brittle systems has also been described from a phenomenological viewpoint [18]. In this case, during the milling, the ductile powders acquire elongated shapes, while the brittle counterparts are simply reduced in size (fig. 5a). The ductile grains become embedded in the brittle matrix, forming a fine dispersion. Further increase of the milling time allows the ductile lamellae to become closer and thinner while the brittle particles become more and more tiny. This is the typical microstructure developed after milling inorganic nanoparticles with polymer matrix [72,73]. The average particle size that can be obtained depends on the relative ease from which the agglomerates can be formed, deformed, fractured and welded. When a large number of fine particles are produced, the degree of refinement is very high. If the particles are rough, spongy, or have their surfaces covered with asperities, strong level of agglomeration takes place [73]. Sometimes, depending on the relative solubility of the precursors, the final product becomes completely homogenized.

5. Mechano-chemistry of polymers

The mechanism by which the mechanical work is converted to chemical energy is really complex and up to date not completely identified [74]. Several modes of energy dissipation are involved in the mechano-chemical reactions. Intermediate thermal energy conversions as well as plasma formation and electromagnetic processes were suggested in literature [67,75–77]. In general, the chemical reactions that can occur on macromolecules subjected to mechanical forces can give up new spatial disposal of atoms, functional groups and conformational changes. Generally, a number of irreversible multistages characterize these processes. Three fundamental steps can be identified: activation, cracking and condensation. The study of the multistage character of the mechano-chemical process showed that the determining step is the cracking, which represents the first step for the mechanical degradation of the macromolecules. On the contrary, the stage of activation takes place at a much lower rate than the other steps and, consequently, it can not be clearly distinguished. Irrespective of the stages of the mechano-chemical process, a number of free radicals are produced; these might initiate many chemical reactions such as grafting, block copolymerization, cross-linking etc. In addition, the stabilization of free radicals is followed by the formation of new functional groups, which are able to promote condensation and/or complexation reactions [78]. In principle, there are two limiting situations (figure 6):

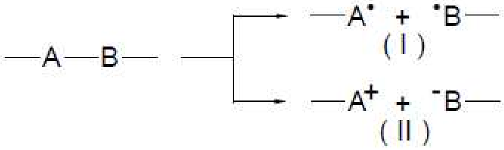

Figure 6: Mechanisms of the mechano-chemical processes.

In the first case the energy consumption is equal to the bond resistance A-B. In the second case the introduction of additional amount of energy, which is equal with the difference between the ionization potential of the fragment -A, and the affinity for the electron of the particle B-, is imposed. Therefore, it is expected that the majority of macromolecular or organic compounds will be split into radicals or molecules, and generate only a small number of active ionic centers. The primary active center mainly considered for the explanation of the majority of reaction mechanisms is the free radical (mechano-radical). The chemical reactivity of the mechano-radicals is governed by the existence of an unpaired electron at the scission place and by the macromolecular dimension [79]. Thus, a high macro-radical length implies a reduced motility, which will determine the subsequent possibilities of conversion. To allow a chemical reaction the active centers must approach each other. Apart from gaseous and liquid states, in the solid state the lifetime of particle pairs and their contact time are high enough. An equilibrium, on all degrees of freedom, must be established between two particles. In these conditions, each pair of active centers represents a particle having its own independence. In literature are reported radical and ionic species, free radicals, and all other active centers formed in mechano-degradation and fracture processes, that are able to initiate reactions of homo- and copolymerization, as well as grafting and block-copolymerization [66]. The pair represents entities with high lifetime and implied in a series of elementary physical steps that are related to rotation, translation, orientation movements, until the occurrence of chemical reaction. The elementary steps of a transfer motion in the solid state require higher activation energies as compared to the same transformations in the liquid or gaseous state. In the first case the transformations occur at much higher surface potentials that those corresponding to the liquid or gaseous states. At the molecular level, the mechano-chemical transformations evolve in the sense of polymer average molecular weight decay and the generation of free radicals. If the formation of radicals is followed by their reaction with the adjacent chains, the net result being the network formation. The dynamic competition between chains breaking and chemical cross-linking is related to the polymer chemical nature, its physical state and the environmental medium nature (inert, presence of reticulation agents, etc.). The existence of the weak bonds, macromolecular chains geometry (i.e. linear, branched, and cross-linked), chains rigidity are other factors that governs the efficiency, kinetic, and mechanism of chains breaking [66]. The morphology of the starting material, also, plays a very important role. In a linear amorphous polymer below its glass transition temperature, the statistically coiled macromolecules tend to uncoil and orient in the loading direction. Due to the strong macromolecule interaction as well as steric hindrance, the stress magnitude must be high in order to reach a fully stretched and elastic tensioned state (above the yield limit) [80]. When the macromolecular chains are organized in a semi-crystalline matrix or in a strong physical network having high values of the relaxation time, their movement will be impeded [80]. In this state, the highly tensioned state can be attained at low level of deformation. The deformation takes place mainly in the so-called disordered zone, which is intercalated between the crystalline blocks of consecutive lamellae [81]. In that case, not all the crossing macromolecules that traverse the amorphous phase connecting the crystalline blocks are fully stretched (fig. 6). During the gradual movement of the crystalline blocks, under the action of an external tensile force, the shortest linking macromolecules will be the first ones to be stretched until the molecule reaches its maximal possible length [82]. In this state, the homolytic scission of macromolecular chains occurs, the stress is integrally redistributed and new macromolecular chains became in a fully extended conformation. It means that the number of split macromolecules, and thus the free radicals, increase with the increasing of sample deformation.

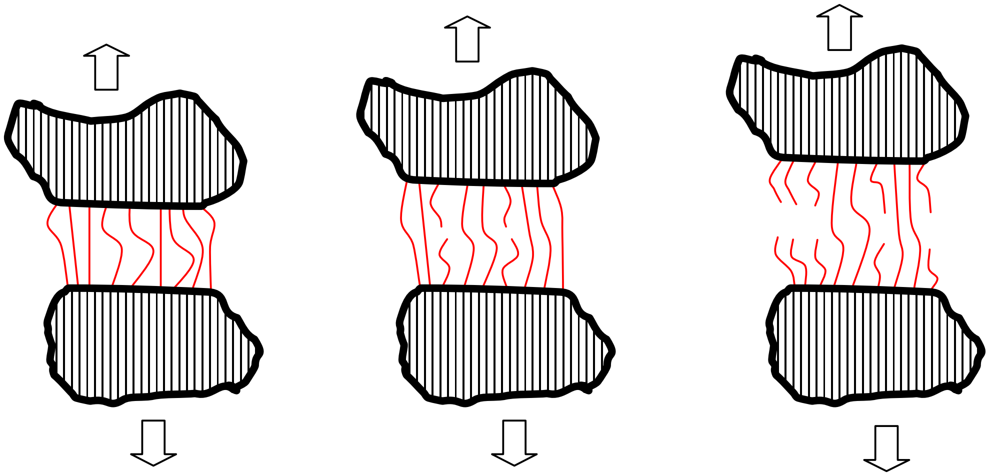

Figure 7: Deformation and fracture of the polymer chains in a semi-crystalline polymer matrix [66].

The influence of the polymer chemical structure on the limit and rate of mechano-degradation is illustrated in Table 1 [66].

Table 1: Influence of the polymer chemical structure on the destruction limit and rate constant [66].

Polymer	**Molecular weight limit** M_L	**Destruction rate constant** (h^{-1})
Cotton cellulose	24462	0.5024
Reed cellulose	22032	0.3470
Viscose	25275	0.1590
Poly (methyl methacrylate)	9000	0.1200
Polystyrene	7000	0.0945
Poly(vinyl acetate)	11000	0.0468
Poly(vinyl alcohol)	4000	0.0237
Cellulose triacetate	10000	-

Several works addressing the structural changes induced by milling in semi-crystalline polymers and their blends are present in literature [17,66,83–85]. Similar reports showed that polymers undergo either a crystalline phase transitions or a simply amorphization when are subjected to mechanical milling [86]. Milling overcomes some problems associated with conventional blending methods such as thermal degradation due to excessive heating in the melting process, or the difficulty in removing the polymer from the solvent if the solution method is used [71].

6. Bio-nanocomposites

Bio-nanocomposites represent a unique integrated class of a research area that covers chemistry, biology, materials science, engineering and nanotechnology. They are becoming increasingly worldwide because they possess extraordinary structural and functional properties [87]. Selecting a suitable matrix and filler it is possible to project new materials to achieve the target field. To generate environmentally friendly materials, as well as to decrease the dependence from the fossil based resources, several biopolymers has been developed in recent years [88,89]. As the properties of such materials are sometimes inferior to the commercial non-biodegradable polymers, nanocomposites of such biopolymers have been developed to improve performances and functionalities. In particular, the choise of the filler is crucial for improving one or more of the inherent limitations related to the biodegradable polymers. The poor processability, moisture and gas barrier, electrical, thermal and physical properties can be altered by the addition of suitable nanoparticles. Polymers which are finding increasing use in the composite technology to replace the non-biodegradable polymers include starch, cellulose, poly(lactic acid), poly(hydroxy alkanoates), pectin, chitosan, etc. The other polymers which though have fossil based sources, but are still biodegradable, include poly(caprolactone), poly(butylene succinate) etc. Significant improvements in the physical performances have been reported in such bio-nanocomposites as compared to pure polymers. Thus, bio-nanocomposites represent potentially high value materials of the future. Nanocomposites containing biopolymers in place of oil-derived polymers need a significant change in the preparation methods, properties, and functionalities of the materials [90–94]. This is due to notable differences in the chemical and physical characteristics between oil-derived polymers and biopolymers. The majority of the biopolymers are not thermoplastic because of their decomposition before melting. As a result, methods like extrusion, widely applied in the case of oil-derived polymers to prepare nanocomposites, are unusable for many biopolymers. The differences between them are also the biocompatibility and biodegradability, which determine distinctions in the areas of their applications. It is worth noting that a great advantage of polymers from renewable resources is that they are widely abundant and at relatively low-cost. Surplus agricultural products, food, industrial and domestic wastes can serve as the source for their production. The particular sensitivity to humidity and high temperatures represents a not negligible problem for the processing scale-up. In some cases it is necessary to unfold the complex macromolecules through denaturation. This is generally done by using chemical denaturants and/or plasticizers consisting of low molecular weight molecules. The additives help to break the numerous intra-molecular interactions, reducing the molecular weight and lowering the glass transition temperature. This enables processing below the decomposition temperature. This means that traditional polymer processing, like extrusion and injection molding, are generally difficult to apply to biodegradable polymers. However, the potential of these materials are, up to now, not completely explored and then very attractive. The distinctive biocompatibility and biodegradability can open the way to new and unpredictable applications. Furthermore, the environmentally responsible handling of large volumes of industrial and agricultural waste materials, such as crop residues, poses a growing problem [95,96]. As the options of disposal and incineration become increasingly less viable due to cost and environmental concerns, a wide variety of methods have been investigated to use these materials as source for biodegradable polymer materials [96–98]. In this context, mechanical milling can produce interesting results by decreasing the molecular weight, promoting amorphization and molecular orientation, and inducing chemical cross-linking [26]. A combination of molecular scission and free radical formation suggests the possibility to break down crop waste and concurrently produce chemically active surfaces, which could be used to produce polymer alloys with novel and useful properties [99]. This possibility is particularly interesting due to the strong market request of low cost biodegradable polymers, including that obtained by natural and waste source [99–101].

7. Nanofillers

Several nanoparticles were proposed as filler into the biodegradable polymer matrices with the aim to improve their physical properties. Change in rheological, thermal, electrical, optical and magnetic properties was reported in literature [91]. The processability, biodegradability, chemical reactivity and durability can be affected as well [1,102]. These numerous modifications are determined by the interactions between the surface of the filler nanoparticles and the polymer matrix. It not surprising that nanofiller shape and dimensions are crucial for the preparation and final properties of bio-nanocomposites. However, highly extended surface area provides an extraordinary abundance of interactions with the matrix [10]. Consequently, a significant effect of nano-fillers can be observed also at very low content. Five main categories of nanofillers are considered in the present review: Layered clays, Carbonaceous fillers, Lignin, Cellulose materials and Halloysite nanotubes.

The most used nano-platelets applied in bio-nanocomposite formulations are the layered or plate-like clay minerals [91,102]. They possess a large aspect ratio because of the thickness of about one nanometer and the width or diameter ranging from tens nanometers up to a few micrometers. In addition, the low cost and the relative abundance in nature make these materials very attractive from technological point of view. Some inorganic nano-clay minerals, such as synthetic layered double hydroxides (LDH), are negatively charged. This represents a challenge to combine them with anionic molecules, which in turn are the most abundant between functional materials (i.e.

antimicrobials, antibiotics, etc.) [103,104]. The LDH structure is similar to that of brucite mineral, a magnesium hydroxide easy to find in nature. In this mineral Mg atoms are octaedrically coordinated to six Oxygen atoms belonging to six groups -OH; each -OH group is, in turn, shared by three octaedrical cations and points the Hydrogen atom to the interlayer space. When some of Mg(II) cations are isomorphously replaced by Al(III) cations, the substitution generates positive charges that are counterbalanced thanks to the presence of counter ions located in the interlamellar regions. The possibility to substitute these anions by simple ionic exchange procedure makes the hydrotalcites ideal solids to be used as host of potentially active molecules having a negative charge. LDH can be prepared with simple procedures and high level of purity, they are also economic and eco-compatible. In the last years, fillers carbon based received a great attention from basic and applied research. Among these, the most interesting are the carbon fibers (CFs), the carbon nanotubes (CNTs), and the graphene nano-platelets (GNPs) [105]. Due to their peculiar characteristics, dimensions and morphologies, they resulted very attractive to produce novel nanocomposites with specifically improved mechanical and electrical properties [106,107]. Cellulose nano-whiskers (CNWs) are highly crystalline materials produced by the acid hydrolysis of natural cellulose [108,109]. The remarkable Young's modulus, high surface-to-volume ratio, and great bending strength make them potential reinforcing fillers in several biodegradable matrices. Lignin is another bio-based filler and represents together with starch, cellulose and hemicellulose the must abundant renewable material on the earth [110,111]. It is generally obtained as a by-product in paper industry through separation from cellulose fibers. Its morphology depends on the kind of process used for delignification [112,113]. New strategies are under continuously investigation with the aim to obtain less altered lignin molecules. For example, steam exploded lignin have proven to be an attractive economic, high performance filler [114]. Very recently, a new class of silicates is drawing attention as fillers for polymers; it is represented by natural halloysite nanotubes (HNTs). Halloysite is two-layered aluminosilicate clay, $Al_2Si_2O_5(OH)_4$ x nH_2O, which exhibits a predominant form of hollow tubes, and it is chemically similar to kaolin. Halloysite dimensions are external diameter of 50-80 nm, lumen of 10-15 nm and length of about 1000 nm. Due to the tubular shape and reduced surface hydroxyl groups, halloysite can be readily dispersed in polymers. In addition, it is possible to use these tubes as containers for release specific active molecules (anticorrosion, antimicrobial, drugs, flame retardant, micro-crack self-healing…) in particular environments [115,116].

8. Conventional methods for preparation of bio-nanocomposites

The complete disaggregation and homogeneous dispersion of fillers into polymer matrix is a prerequisite to obtain a nanocomposite with the desidered properties [1,117]. Therefore, the method of preparation is of a basic importance. Up to now, four different approaches are commonly used to fabricating nanocomposites. They will be shortly introduced and discussed below.

8.1 Solution method

In solvent processing the biodegradable polymers are dissolved in a suitable solvent and then mixed with the nano-filler [118]. High temperatures are often required for reducing quantity of solvent and reducing the time necessary for the complete solubilization of the polymer. After a complete homogenization of the solution, it is casted into a film by spreading or casting it on a flat surface and allowing the solvent to evaporate. To speed up the process of solvent removal and subsequent plastic hardening heat is applied along with controlled forced convection. It is important to have an idea of the molecular interactions of the polymer with the solvent. A poor compatibility, as well as a strong affinity, can lead to uncontrolled precipitation or heterogeneous morphology with poor distribution of the nano-sized particles. This method is a common laboratory practice with limited applications to large scale production. The reasons are the numerous drawbacks that the use of high quantity of solvents includes. In fact, they are generally expensive and sometime toxic. Large quantities of heat are required to evaporate the solvent. Articles with controlled thickness and complex designs cannot be made. The process is generally time consuming and requires specialized equipments.

8.2 Melt mixing

The melt-mixing technique is the traditional method applied to the thermoplastic materials [119]. It is relatively inexpensive, does not require the use of potentially harmful volatile solvents, and a cost-competitive process for high-volume production. Unfortunately, it is not always suitable for natural polymers, which undergo thermal degradation phenomena at temperature above the melting. In some cases, however, it is possible to use appropriate plasticizers that are able to convert biodegradable polymers like starch or protein into a thermoplastic-like state [120–122]. The plasticizer increases the chains mobility, reduces the intramolecular interactions and lowers the softening temperature of the biodegradable materials. It allows to process the materials at lower temperature and with lower mechanical energy necessary for mixing, consolidate and shaping. After that, the composite is cooled down to the ambient temperature, where the material "solidifies" in a more rigid structure. The mechanical characteristics of the resulting composites, however, are strongly dependent by the plasticizer type and concentration. Some of the properties are too poor to completely hinder any other improvement introduced by the nanofiller. In addition, it is not possible to avoid the natural migration of the low molecular weight plasticizers from the polymeric material. Migration leads to stiffer and less extendable polymers, increases the permeation of oxygen and the diffusion of moisture. Sometime, the risk of leaching out of certain plasticizers, such as phthalates, during storage or end-user application, constitutes another important limitation of this technique [123].

8.3 In situ polymerization

Liquid monomer or monomer solutions are generally used to first disperse the nanoparticles. The polymerization is performed thereafter [124]. The method, undoubtedly, represents the basic technique in nanocomposite preparation, but it is impossible to realize with the majority of natural polymers.

8.4 Template synthesis

Template synthesis involves the synthesis of inorganic material in the presence of polymer matrix. Bio-molecules, parts and whole cells, microorganisms are used as the template for inorganic materials that are generated from a precursor [125,126]. It can be possible to synthesize as nano-sized particles, coating or shell and mesoporous matrix in which templating bio-molecules are entrapped. Such technique is highly versatile, being adapted for many different bio-nanocomposite preparations. The inorganic component is often synthesized by sol-gel chemistry methods [127–129]. The bio-mineralization processes of living cells are reported as an example of large scale fabrication [130]. Furthermore, there is a problem in the template synthesis of biomaterials because of their incompatibility with the common sol-gel processing [131,132], which restricts opportunities to bio-mimic the bio-mineralization processes of living cells.

9. Bio-nanocomposites prepared by mechanical milling

The mechanical milling is an interesting sustainable alternative to achieve homogeneous dispersion of nano-fillers into polymers [133]. Recent publications have shown the possibility to use the milling for coating inorganic nano-particles [134,135]. Additional examples are the mechanical degradation of rubbers [136] and thermoset polymers [137]. Milling can be utilized for chemical modification of already existing polymers [138] or for block-polymerization [139]. In that case, the mechanism of polymerization is not much different from that used in compatibilization by reactive extrusion: radicals recombine with each other. Another advantage of the mechano-chemical route is the possibility of parallel processes (surface grafting, embedding, polymerization, compatibilization) that proceed at very high specific energy. It is particularly suitable in the case of biodegradable polymers, either from fossil or from renewable sources [140]. For example, waste disposal and recycling are already existing application for the mechanical milling [28,136]. In that case, the mechanical forces imposed by the grinding medium allow the dispersion and compatibilization of the “active” phase (filler) into the polymer matrix. At the same time, the thermal and mechanical degradation can be strongly limited by controlling the processing conditions such as the temperature, the milling time and the grinding media [141]. In additions, the possibility to form in situ the nanoparticles and to promote chemical reactions between both the organic molecules and the activated filler nanoparticles represents another indubitable advantage of this method. Surface activation and simultaneous treatment allow the production of active fillers from the otherwise intractable crop waste materials. Furthermore, the possibility to conduct the process in dry conditions is important not only for ecological issues, but also for safety reasons.

9.1 Bioplastics from fossil based resources

Bugatti et al [142] demonstrated that the mechanical milling is a simple way to reduce “active” particle size, and thus enhance their antimicrobial effect. They prepared a LDH modified with antimicrobial salicylate anions by a direct co-precipitation method. The mean dimensions of the pristine LDH-salicylate (25 μm) were strongly reduced by milling treatment of the powders. In particular, after 1, 2 and 5 minutes of milling were obtained 16, 9.9 and 8.2 μm, respectively. SEM analysis showed that the starting irregular agglomerated morphology became uniform and smaller after milled. Comparing the release kinetic of salicylate anion from powders with different dimensions, they found a monotonic increase with the lower powder dimensions. The antimicrobial activity agains *E. Coli* was found dependent on particle size, and in particular, much more efficient for the sample obtained with higher milling time (Figure 8). These results clearly indicated that it is possible to modulate the release kinetics and the antimicrobial activity of the LDH system by changing the milling conditions [142]. Sorrentino et al [15] reported the preparation of nanocomposites based on poly(ε-caprolactone) (PCL) and a Mg-Al layered double hydroxide (LDH), organically modified with 12-hydroxydodecanoate anion (HAD). They evaluated the effect of ball milling on the molecular weight and molecular weight distribution of the commercial used PCL. A decay of M_w from 195 KDa to 96.3 KDa, after 30 mins of milling were observed. The PDI (M_w/M_n) varied from 2.54 to 3.50 after 30 mins of milling. A comparison between the mechanical properties of the not-milled PCL [143] and mechanical milled one [15] is reported in table S1 of supporting materials. After milling, the elastic modulus resulted slightly worse, but still acceptable for a thermoplastic material, while the other analyzed mechanical parameters appeared unchanged, or even improved.

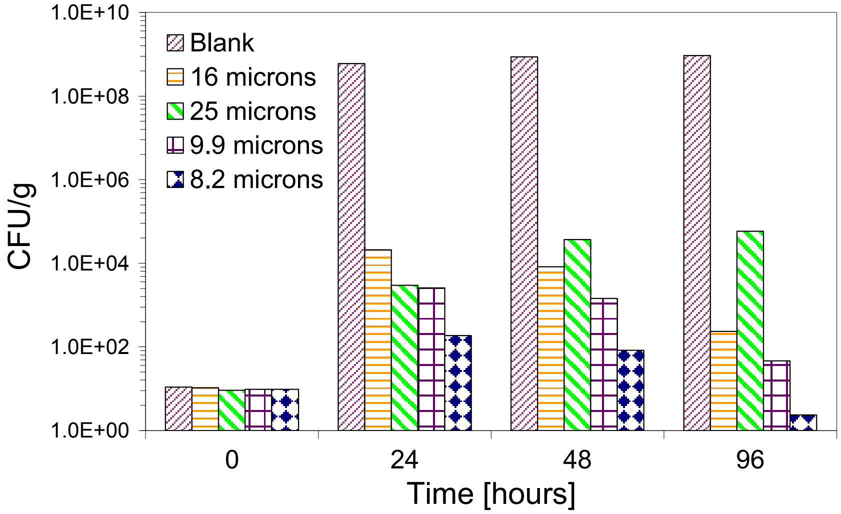

Figure 8: Evolution of *E. Coli* in the presence of 4% (w/v) solution of ZnAl-o-BzOH powders as function of filler dimension and contact time. Data adapted from ref [142]

Romeo et al. [144] reported the mechanical milling preparation of PCL nanocomposites filled with a LDH, and LDH organically modified with 12-hydroxydodecanoic acid (LDH-HA). The composites were submitted to the electrospinning process. The morphological analysis showed that the pure PCL developed fibers with an average diameter of 600 ± 50 nm. The addition of LDH, that remained almost unaffected by the milling, did not change the fiber dimensions. At variance, the fibers with the organically modified LDH-HA showed a significantly lower average diameter in the range of 300 ± 50 nm. In that case, the inorganic lamellae were exfoliated and residing inside the nanofibers, as shown by X-rays and EDX analysis. Pucciariello et al. [145,146] reported the preparation and characterization of composites PCL/Lignin prepared by high energy ball milling, in a wide range of composition. Table S1 in the supporting materials reports the mechanical parameters evaluated on some selected nanocomposites containing different lignin type and loading [145,146]. It was concluded that the highest elastic moduli were reached by composite filled with 30 and 40 wt% of sulfonated lignin. Costantino et al. [147] and Bugatti et al. [148,149] reported the preparation and the characterization of biodegradable active polymer films by means of mechanical milling. The composites were considered as model for “active packaging” systems. Firstly, the following antimicrobial molecules were intercalated into LDH: Benzoate (Bz), 2,4-dichlorobenzoate (BzDC), para- and ortho-hydroxybenzoate (p- and o-BzOH). The resulting powder were mixed with PCL by means of an high energy ball milling. Finally, polymeric films were obtained by hot-pressing the milled powders. The chemical and stereochemical structure of the active molecule, as well as the milling process, developed different composites' morphologies. Antimicrobial tests indicated that the composites were able to inhibit the *Saccharomyces cerevisiae* growth up to the 40%. The kinetic release of the benzoate molecules and of the p-OH benzoate molecules, dispersed in PCL either anchored to LDH or mixed to PCL, is shown in figure 8 as function of time ($h^{0.5}$).

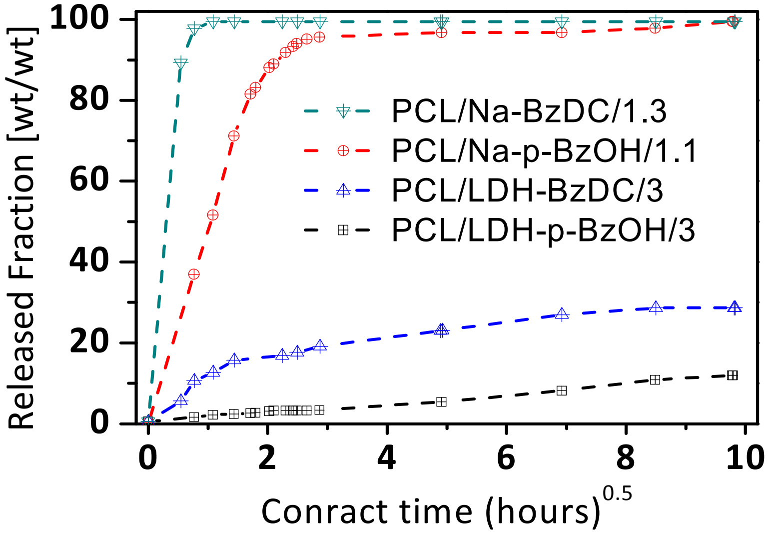

Figure 9: Release fraction as a function of the time. Data adapted from ref [148,149].

It was observed that the release of active molecules from the lamellar solid incorporated into the polymeric matrix was much slower than the release of them simply blended to the PCL. The type of active molecule, its percentage, and the milling conditions can be used for tuning the kinetic release to the specific applications [148,149] . Vertuccio et al. [150] reported the influence of ball milling conditions on the structure and physical properties of PCL/Starch/Clay composites. The used milling conditions did not influence the PCL crystalline structure, neither when it is pure nor in blends with starch and clay. In the supporting materials (table S1) are summarized all the mechanical properties of the discussed samples. The best mechanical and barrier (table S2 in supporting materials) performances of PCL/LDHs nanocomposites were achieved by 2.8 wt% of Mg-Al hydrotalcite modified with 12-hydroxydodecanoic acid. Such molecule ought the best compatibilization between the two phases, improving the physical properties of the nanocomposite at low filler loading. Better increasing in PCL stiffness, in terms of elastic modulus, was employed by milling with starch and 3 wt% of Clay. The improvement increased with milling time. On the contrary, very weak elongation parameters were detected. The increase in the modulus was attributed both to a better interfacial adhesion between the PCL and starch, and the reinforcement effect from the dispersion of the clay in the matrix. Better interfacial adhesion was associated with the formation of cross-links, starch-starch, PCL-PCL and starch-PCL.

Barrier properties to water vapor, in terms of diffusion, resulted slightly worsened for pure PCL, for the molecular weight decay inducted by the milling processing [15]. Furthermore, the bio-nano-composites, with different lamellar fillers, and different filler loading delayed the diffusion of water vapor to a large extent. This phenomenon was correlated to the exfoliation of the clay: the more extended was the clay delamination the lower resulted the diffusion coefficient (table S2 in supporting materials). Cocca et al.[151] reported the use of cellulose particles, obtained through a solvent-free mechano-chemical process, as filler for biodegradable composites based on PCL. Commercial cellulose fibers, having different lengths, were also tested. PCL modified with maleic anhydride was used to better compatibilize the two phases. Composites were tested through physico-mechanical characterizations, in order to evaluate the influence of cellulose structure and morphology and polymer/filler interfacial adhesion on the final properties of the materials (table S1 in supporting materials). The use of the amorphous cellulose particles combined with the presence of a suitable interfacial agent allowed to modulate important technological properties of the composites, such as tensile and thermal properties, water absorption, water vapor transmission rate and biodegradation kinetics. For all the composites, a reduction of this parameter was recorded with respect to neat PCL. Nevertheless, when medium length cellulose fibers were used as filler, the drop of the elongation at break already occurred at 20 wt% filler loading, whereas in the case of amorphous cellulose, the ductile behavior of the material was preserved also at the highest content of filler. The sample containing 30 wt% of amorphous cellulose still showing a noticeable elongation at break, higher than 300%.

Santangelo et al. [152] , Gorrasi et al. [153] reported the preparation by ball milling and characterization of nanocomposites based on Poly(L-lactide), CNTs-Fe/clay and CNTs-Fe/Na^+-clay hybrid fillers, synthesized by direct Catalytic Chemical Vapor Deposition (CCVD) over clay-based catalysts. PLA composites showed improved physical properties with respect to the pristine polymer. The conductive component (CNTs) was responsible for the significant conductivity enhancement (up to 9 orders of magnitude) with respect to the insulating PLA ($\sigma=1\cdot10^{-10}$ S/m). The percolation threshold of the PLA/Clay-CNTs hybrids resulted less than half than the percolation threshold showed by the nanocomposites filled with neat CNTs [153] (fig. 10). The experimental results suggested that clay and CNT had a synergistic action in improving the polymer physical properties. In particular, PLA-CNTs-Fe/Na^+-clay exhibited better performance than PLLA-CNTs-Fe/clay. Such a difference was explained as the effect of the lower degree of graphitization and the minor level of bundling of the CNTs formed over Fe/Na^+-clay. The latter factor was indicated as responsible for a different degree of dispersion of the CNTs-Fe/Na^+-clay filler inside the PLA matrix.

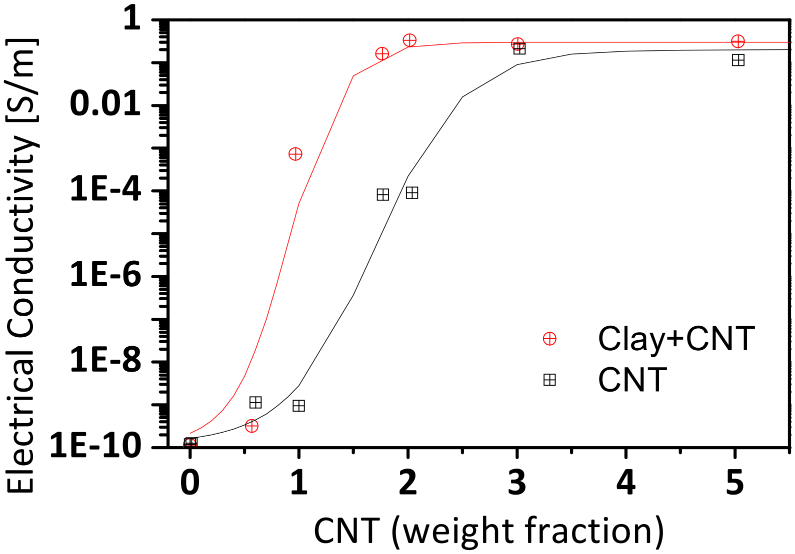

Figure 10: Electrical conductivity as a function of the CNT content. Data adapted from ref [153]

9.2 Bioplastics from renewable sources

Kim et al. [154] reported the preparation of nanocomposites based on single walled carbon nanotubes (SWNTs) and Poly(L-lysine), using high speed vibration milling. Longer ball-milling time treatment was considered to induce disorder within the bundles and fracture the nanotubes. On the contrary, shorter milling time (5 min) treatment reduced the length of SWNTs. The authors concluded that after grinding in a mixer mill, the SWNTs are fully covered or wrapped with the poly(L-lysine) polymer. The molecular model suggested that the free amino groups of polymer are adsorbed or interact strongly on the SWNTs surface. This adsorption or wrapping allowed a high surface area coverage with low backbone strain around the nanotubes. The authors suggested that a weak, long-range entropic repulsion among polymer-attached tubes acted as a barrier that prevents the tubes from approaching the attractive parts of the inter-tube potential. Avolio et al. [47] reported the effects of a dry ball milling process on the cellulose structure, morphology and properties. The total energy transferred to the cellulose was calculated through a kinematical model as a function of the milling time. They found a value ranging from about 102 kJ per mol of β-d-glucopyranose units (2 min milling), up to about 3060 kJ per mol of β-d-glucopyranose units (60 min ball milling). As consequence of the ball milling treatments, the average length of the fibers decreased from an original value of about 200 μm up to about 12 μm, after 60 min ball milling. The original fibrous morphology of the cellulose was modified to a quasi-circular shape. During the first stages of ball milling (up to 15 min) the diameter of the fibers was quite unchanged, whereas after 30 min ball milling the almost complete disappearance of the fibrous structure was evidenced with the formation of amorphous cellulose micro-particles. As effect of the cellulose amorphization, the amount of absorbed water increased from 7.3 wt% for untreated cellulose up to 11.6 wt% for the sample milled for 60 min. This behavior confirmed that water can be easily absorbed by the amorphous fraction, whereas crystalline domains are less accessible to water molecules. Mangiacapra et al. [155] reported the preparation of composites based on apple peel pectin with 3 wt% of either a natural (MMT) or an organically modified montmorillonite (OMMT) clay, using ball milling. The mixed powders were water cast as films, and then characterized. The absence of the peak corresponding to the basal spacing of the clay in the X-ray diffractograms of the composite samples suggested the exfoliation of the clay. Gorrasi et al. [156] reported the preparation and characterization of novel nanocomposites of apple peel pectin with 5 wt% of nano-hybrid fillers based on layered double hydroxide (LDH) containing molecules with antimicrobial activity: benzoate (Bz), 2,4-dichlorobenzoate (DCBz), para hydroxybenzoate (p-OHBz) and ortho hydroxybenzoate (o-OHBz). Composites were prepared through ball milling in the presence of distilled water. Milled composites were casted and analyzed. Thermogravimetric analysis showed that the presence of the nano-hybrids allowed the pectin matrix to degrade at higher temperatures. Composite films showed antimicrobial activity (figure 11), indicating the potential application in the packaging field and opening new perspectives in using pectins-antimicrobials as green coating agents for a wide number of packaging polymers.

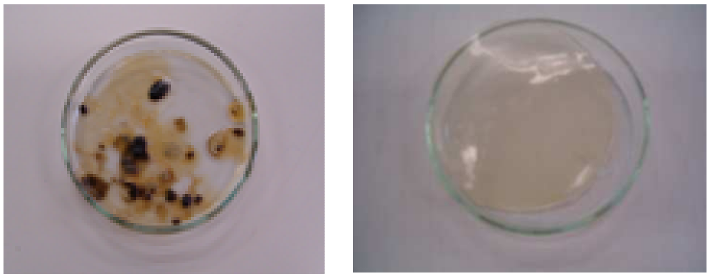

(A) (B)

Figure 11: Pictures of film of unfilled pectin (A) and composite with 5 wt% of LDH-p-OH-Bz (B) after 12 months of storage at ambient temperature, adapted from ref [156]

Gorrasi [157] reported the development of novel green biodegradable nanocomposites based on pectins and a nano-hybrid (NH) composed of natural halloysite (HNTs) and rosemary oil. Essential oils, applied to the formulation of edible films, provide them with antioxidant and/or antimicrobial properties. TGA analysis allowed to hypothesize that the HNTs entrapped oil molecules into their lumen. X-ray analysis on the composites showed that pure pectin presented an amorphous structure, which is retained in all the composites. The basal peak of dehydrated HNTs disappeared and/or expanded after the intercalation of essential oil. The mechanical properties, in terms of elastic modulus, were significantly improved for composites with 5 and 10 wt% of NH. The reinforcing effect of NH was evident also for stress at break, especially at low NH content. The lower was the nano-hybrid percentage the better the dispersion of the filler into the organic phase. By increasing the percentage of filler in the composites (i.e. 20%), the formation of "clusters" occurred, thus determining a deterioration of the mechanical parameters. Barrier properties, in terms of diffusion of water vapor, resulted improved. The thermodynamic diffusion coefficient decreased on increasing the nano-hybrid loading (figure 12). The presence of the filler increased the tortuosity of the system, leading to a decrease in the value of the diffusion coefficient.

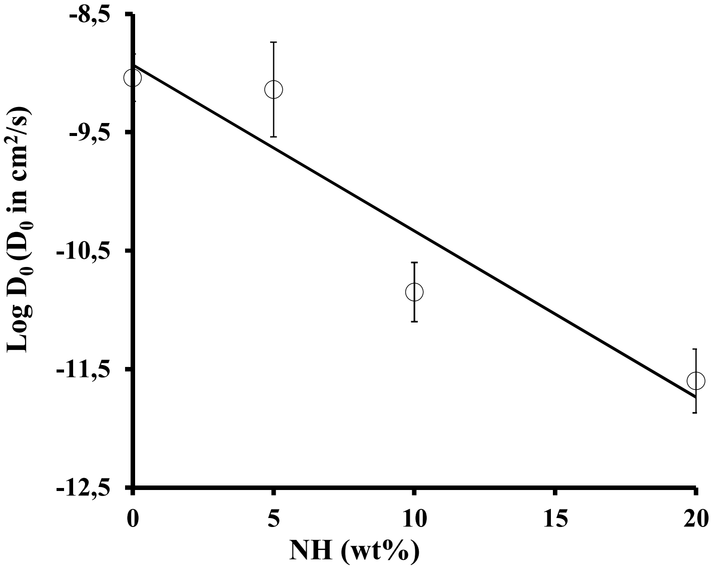

Figure 12: Thermodynamic diffusion parameter, as function of Nano-hybrid (NH) loading, adapted from ref [157]

A comparison of the molecular release of the rosmarinic acid molecules directly dispersed in pectins and in the nano-hybrid was analysed, indicating the much slower release in the latter case (Figure 13)

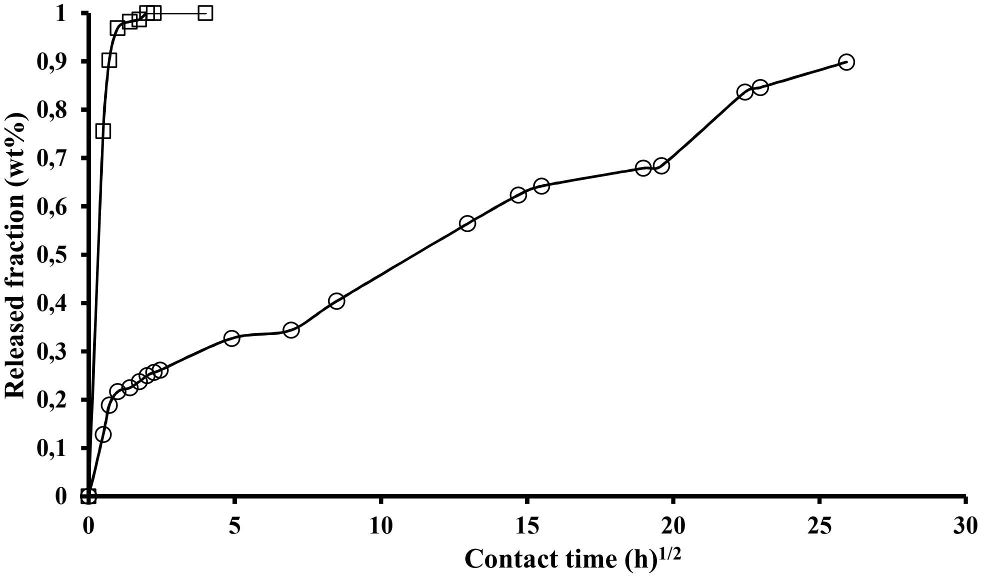

Figure 13: Rosmarinic acid released fraction (wt/wt%) as function of contact time (h)$^{1/2}$ for: Pectin and 15 wt% of rosemary oil directly dispersed into pectin (□) and HNTs loaded (○), adapted from ref [157].

The better modulus was achieved with 3 wt% of MMT and was attributed to the strong interactions between pectin matrix and silicate layers via formation of hydrogen bonds (table S3 in supporting materials) [155–157]. The organic pendants of the OMMT filler probably created an interface between clay sheets and pectin molecules hindering, or reducing, the formation of hydrogen bonds between them. In the case of LDHs fillers, the highest modulus was reached for composites with LDH/p-OHBz, probably for stronger interactions between pectin matrix and nanohybrid layers via formation of hydrogen bonds, better favored by the p-OHBz molecule. For pectin filled with HNTs loaded with rosemary oil, and plasticized with glycerol are observed the worst moduli. This is due either to the plasticizing effect of glycerol or to the lubricant action of rosemary oil free molecules dispersed into the pectin matrix.

The best barrier performances, for LDHs composites, were employed with p-OHBz host molecule, confirming that the interaction filler-polymer phase had an important influence also on diffusion of water (table S4 in supporting materials) [155-157]. Bio-composites filled with HNTs loaded with rosemary oil showed the best barrier properties, in terms of diffusion. This can be due either to the halloysite nanotubes high loading and dispersion into the pectin matrix, or to the incompatibility between penetrating water molecules and oil free dispersed molecules, acting themselves as barrier agents.

Hassan et al. [101,158] explored the possibility to utilize waste eggshells and sea shells (littleneck, quahog clams and mussels) as raw material to produce high surface area biocalcium carbonate nanoparticles using a combination of mechano-chemical and ultrasonic irradiation techniques. Their results showed that ball milling is an efficient method for size reduction of sea shells to produce smaller size particles [158]. In particular, they demonstrated that the incorporation of bio-CaCO3 nanoparticles derived from eggshells in a thermoplastic biodegradable polymer (Bioplast GS 2189) increased both thermal and mechanical properties [101].

10. Trends and Perspectives

The introduction of novel functionalities into bioplastics, either from renewable or fossil sources, by means of mechanical milling is one the greatest challenges of science and technology of materials. The mechanical milling has been demonstrated to be an efficient and green technique for the production of polymeric bio-nanocomposites with advanced structural and functional properties. The possibility to avoid solvents and high temperatures contains within itself several advantages. In fact, the utilization of solvents (i.e. solvent casting techniques) generates inevitable disposal and environmental problems. The use of high temperatures and shear stresses (i.e. melt blending techniques) can cause degradation in polymers. In addition, high temperatures are not suitable for the processing of natural polymers that undergo degradation with temperature. Therefore, the main advantages, in comparison with the traditional technologies, are the simplification of the processes, ecological safety and decrease in the number of technological stages. Furthermore, for the production of composites having thermo-sensitive active molecules (i.e. antimicrobials, oxygen scavengers, antibiotics, anti-inflammatory) the processing at high temperatures for long time represents a serious problem. Several issues are still open, and many fundamental aspects of such process applied to bio-polymers need to be investigated and clarified. In particular, a satisfactory modeling of all phenomena that occur during the processing is not available yet. A deep knowledge of all the physical phenomena involved during the mechanical milling can open new and fundamental perspectives in the industrial production of one-pot polymer bio-nanocomposites either by mechanical mixing, or by mechanochemistry and even click-mechanochemistry approach.

References

1 S. Sinha Ray and M. Okamoto, *Prog. Polym. Sci.*, 2003, **28**, 1539–1641.

2 F. Hussain, *J. Compos. Mater.*, 2006, **40**, 1511–1575.

3 A. Sorrentino, G. Gorrasi, M. Tortora and V. Vittoria, *Polymer Nanocomposites*, Elsevier, 2006.

4 M. Alexandre and P. Dubois, *Mater. Sci. Eng. R Reports*, 2000, **28**, 1–63.

5 E. Manias, A. Touny, L. Wu, K. Strawhecker, B. Lu and T. C. Chung, *Chem. Mater.*, 2001, **13**, 3516–3523.

6 P.-C. Ma, N. a. Siddiqui, G. Marom and J.-K. Kim, *Compos. Part A Appl. Sci. Manuf.*, 2010, **41**, 1345–1367.

7 A. Sorrentino, M. Tortora and V. Vittoria, *J. Polym. Sci. Part B Polym. Phys.*, 2006, **44**, 265–274.

8 A. Sorrentino, G. Gorrasi and V. Vittoria, *Trends Food Sci. Technol.*, 2007, **18**, 84–95.

9 E. M. Hotze, T. Phenrat and G. V. Lowry, *J. Environ. Qual.*, 2010, **39**, 1909.

10 G. Schmid, Ed., *Nanoparticles: From Theory to Application, 2nd, Completely Revised and Updated Edition*, Wiley-VCH Verlag GmbH & Co. KGaA, 2010.

11 A. Lerf, in *Handbook of Nanostructured Materials and Nanotechnology. Volume 5: Organics, Polymers, and Biological Materials*, ed. H. S. Nalwa, Academic Press, Burlington, 2000, pp. 1–166.

12 T. Liu, C. Burger and B. Chu, *Prog. Polym. Sci.*, 2003, **28**, 5–26.

13 P. M. Ajayan, L. S. Schadler and P. V. Braun, Eds., *Nanocomposite Science and Technology*, Wiley-VCH Verlag GmbH & Co. KGaA, Weinheim, FRG, 2003.

14 Y. G. Zhu, Z. Q. Li, D. Zhang and T. Tanimoto, *J. Appl. Polym. Sci.*, 2006, **99**, 501–505.

15 A. Sorrentino, G. Gorrasi, M. Tortora, V. Vittoria, U. Costantino, F. Marmottini and F. Padella, *Polymer (Guildf).*, 2005, **46**, 1601–1608.

16 T. F. Grigorieva, a. P. Barinova and N. Z. Lyakhov, *J. Nanoparticle Res.*, 2003, **5**, 439–453.

17 G. Kaupp, *CrystEngComm*, 2009, **11**, 388.

18 C. Suryanarayana, *Prog. Mater. Sci.*, 2001, **46**, 1–184.

19 P. Baláž, in *Mechanochemistry in Nanoscience and Minerals Engineering SE - 6*, Springer Berlin Heidelberg, 2008, pp. 297–405.

20 G.-W. Wang and J. Gao, *Green Chem.*, 2012, **14**, 1125.

21 W. Qiu, T. Endo and T. Hirotsu, *Eur. Polym. J.*, 2005, **41**, 1979–1984.

22 F. Zhang, W. Qiu, L. Yang, T. Endo and T. Hirotsu, *J. Mater. Chem.*, 2002, **12**, 24–26.

23 C. Bai, *Polymer (Guildf).*, 2000, **41**, 7147–7157.

24 S. Jonna and J. Lyons, *Polym. Test.*, 2005, **24**, 428–434.

25 H. Mio, J. Kano and F. Saito, *Chem. Eng. Sci.*, 2004, **59**, 5909–5916.

26 F. Cavalieri and F. Padella, *Waste Manag.*, 2002, **22**, 913–916.

27 V. Gente, F. La Marca, F. Lucci, P. Massacci and E. Pani, *Waste Manag.*, 2004, **24**, 663–72.

28 X. Guo, D. Xiang, G. Duan and P. Mou, *Waste Manag.*, 2010, **30**, 4–10.

29 P. He, B. He, W. Xiao and Y. Zhang, *J. Vinyl Addit. Technol.*, 2006, **12**, 42–48.

30 W. Shao, Q. Wang, Y. Chen and Y. Gu, *Mater. Manuf. Process.*, 2006, **21**, 173–179.

31 K. Awasthi, *Int. J. Hydrogen Energy*, 2002, **27**, 425–432.

32 Y. B. Li, B. Q. Wei, J. Liang, Q. Yu and D. H. Wu, *Carbon N. Y.*, 1999, **37**, 493–497.

33 R. JANOT and D. GUERARD, *Prog. Mater. Sci.*, 2005, **50**, 1–92.

34 C. Lu and Q. Wang, *J. Mater. Process. Technol.*, 2004, **145**, 336–344.

35 B. S. M. Claudio L. De Castro, in *Synthesis, Functionalization and Surface Treatment of Nanoparticles*, ed. M.-I. Baraton, American Scientific Publishers, 2002, pp. 1–14.

36 A. P. Smith, H. Ade, C. M. Balik, C. C. Koch, S. D. Smith and R. J. Spontak, *Macromolecules*, 2000, **33**, 2595–2604.

37 B. K. Mishra, *Int. J. Miner. Process.*, 2003, **71**, 95–112.

38 B. K. Mishra, *Int. J. Miner. Process.*, 2003, **71**, 73–93.

39 C. F. Burmeister and A. Kwade, *Chem. Soc. Rev.*, 2013, **42**, 7660–7.

40 I. Colombo, G. Grassi and M. Grassi, *J. Pharm. Sci.*, 2009, **98**, 3961–86.

41 R. Venugopal and R. . Rajamani, *Powder Technol.*, 2001, **115**, 157–166.

42 R. K. Rajamani, B. K. Mishra, R. Venugopal and A. Datta, *Powder Technol.*, 2000, **109**, 105–112.

43 P. . Chattopadhyay, I. Manna, S. Talapatra and S. . Pabi, *Mater. Chem. Phys.*, 2001, **68**, 85–94.

44 M. Magini, C. Colella, A. Iasonna and F. Padella, *Acta Mater.*, 1998, **46**, 2841–2850.

45 A. Iasonna and M. Magini, *Acta Mater.*, 1996, **44**, 1109–1117.

46 R. A. Varin, T. Czujko and Z. S. Wronski, *Nanomaterials for Solid State Hydrogen Storage*, Springer US, Boston, MA, 2009.

47 R. Avolio, I. Bonadies, D. Capitani, M. E. Errico, G. Gentile and M. Avella, *Carbohydr. Polym.*, 2012, **87**, 265–273.

48 I. Bonadies, M. Avella, R. Avolio, C. Carfagna, G. Gentile, B. Immirzi and M. E. Errico, *Polym. Test.*, 2012, **31**, 176–181.

49 D. Chen, H. yan Liu and L. Li, *Mater. Chem. Phys.*, 2012, **134**, 921–924.

50 N. Poudyal, V. V. Nguyen, C. Rong and J. P. Liu, *J. Phys. D. Appl. Phys.*, 2011, **44**, 335002.

51 F. Li, J.-F. Li, L.-D. Zhao, K. Xiang, Y. Liu, B.-P. Zhang, Y.-H. Lin, C.-W. Nan and H.-M. Zhu, *Energy Environ. Sci.*, 2012, **5**, 7188.

52 D. Chen, Y. Zhang, B. Chen and Z. Kang, *Ind. Eng. Chem. Res.*, 2013, **52**, 14179–14184.

53 S. C. Tjong and H. Chen, *Mater. Sci. Eng. R Reports*, 2004, **45**, 1–88.

54 L. Andrić, A. Terzić, Z. Aćimović-Pavlović, L. Pavlović and M. Petrov, *Compos. Part B Eng.*, 2014, **59**, 181–190.

55 D. L. Zhang, *Prog. Mater. Sci.*, 2004, **49**, 537–560.

56 T. S. Ward, W. Chen, M. Schoenitz, R. N. Dave and E. L. Dreizin, *Acta Mater.*, 2005, **53**, 2909–2918.

57 Q. S. Mei and K. Lu, *Prog. Mater. Sci.*, 2007, **52**, 1175–1262.

58 L. Takacs and J. S. McHenry, *J. Mater. Sci.*, 2006, **41**, 5246–5249.

59 E. V Shelekhov, V. V Tcherdyntsev, L. Y. Pustov, S. D. Kaloshkin and I. A. Tomilin, in *Investigations and Applications of Severe Plastic Deformation SE - 19*, eds. T. Lowe and R. Valiev, Springer Netherlands, 2000, vol. 80, pp. 139–145.

60 J. Joardar, S. . Pabi and B. . Murty, *Scr. Mater.*, 2004, **50**, 1199–1202.

61 Y.-S. Kwon, K. B. Gerasimov and S.-K. Yoon, *J. Alloys Compd.*, 2002, **346**, 276–281.

62 S. Zghal, R. Twesten, F. Wu and P. Bellon, *Acta Mater.*, 2002, **50**, 4711–4726.

63 S. L. James and T. Friščić, *Chem. Soc. Rev.*, 2013, **42**, 7494–6.

64 L. Takacs, *Prog. Mater. Sci.*, 2002, **47**, 355–414.

65 E. Arzt, G. Dehm, P. Gumbsch, O. Kraft and D. Weiss, *Prog. Mater. Sci.*, 2001, **46**, 283–307.

66 C. Vasiliu-Oprea and F. Dan, *MACROMOLECULAR MECHANOCHEMISTRY. Polymer Mechanochemistry vol. 1*, Cambridge International Science Publishing Ltd, Cambridge, 2006.

67 V. V Boldyrev and K. Tkáčová, *J. Mater. Synth. Process.*, 2000, **8**, 121–132.

68 C. C. Koch, in *Materials Science and Technology*, Wiley-VCH Verlag GmbH & Co. KGaA, 2006.

69 P. Baláž, M. Achimovičová, M. Baláž, P. Billik, Z. Cherkezova-Zheleva, J. M. Criado, F. Delogu, E. Dutková, E. Gaffet, F. J. Gotor, R. Kumar, I. Mitov, T. Rojac, M. Senna, A. Streletskii and K. Wieczorek-Ciurowa, *Chem. Soc. Rev.*, 2013, **42**, 7571–637.

70 A. P. Smith, H. Ade, C. C. Koch and R. J. Spontak, *Polymer (Guildf).*, 2001, **42**, 4453–4457.

71 M. Stranz, U. Köster and F. Katzenberg, *J. Metastable Nanocrystalline Mater.*, 2005, **24-25**, 609–614.

72 G. Gorrasi, M. Sarno, A. Di Bartolomeo, D. Sannino, P. Ciambelli and V. Vittoria, *J. Polym. Sci. Part B Polym. Phys.*, 2007, **45**, 597–606.

73 M. Abareshi, S. M. Zebarjad and E. K. Goharshadi, *J. Vinyl Addit. Technol.*, 2010, **16**, 90–97.

74 L. Takacs, *Chem. Soc. Rev.*, 2013, **42**, 7649–59.

75 E. Boldyreva, in *The Future of Dynamic Structural Science SE - 6*, eds. J. A. K. Howard, H. A. Sparkes, P. R. Raithby and A. V Churakov, Springer Netherlands, 2014, pp. 77–89.

76 P. A. May and J. S. Moore, *Chem. Soc. Rev.*, 2013, **42**, 7497–506.

77 K. S. McKissic, J. T. Caruso, R. G. Blair and J. Mack, *Green Chem.*, 2014, **16**, 1628.

78 G.-W. Wang, *Chem. Soc. Rev.*, 2013, **42**, 7668–700.

79 A. Stolle, T. Szuppa, S. E. S. Leonhardt and B. Ondruschka, *Chem. Soc. Rev.*, 2011, **40**, 2317–29.

80 W. Grellmann and S. Seidler, Eds., *Deformation and Fracture Behaviour of Polymers*, Springer Berlin Heidelberg, Berlin, Heidelberg, 2001.

81 I. M. Ward and J. Sweeney, *Mechanical properties of solid polymers*, John Wiley & Sons, 2012.

82 D. Gross and T. Seelig, *Fracture mechanics: with an introduction to micromechanics*, Springer, 2011.

83 W. J. D. Shaw, *Mater. Sci. Forum*, 1998, **269-272**, 19–30.

84 T. Friscic, in *Ball Milling Towards Green Synthesis: Applications, Projects, Challenges*, The Royal Society of Chemistry, 2015, pp. 151–189.

85 T. Hirotsu, T. Endo and M. Umemura, in *Ball Milling Towards Green Synthesis: Applications, Projects, Challenges*, The Royal Society of Chemistry, 2015, pp. 203–240.

86 A. P. Cysne Barbosa, M. Stranz, F. Katzenberg and U. Köster, *e-Polymers*, 2009, **9**, 1–7.

87 L. C. Tomé, R. J. B. Pinto, E. Trovatti, C. S. R. Freire, A. J. D. Silvestre, C. P. Neto and A. Gandini, *Green Chem.*, 2011, **13**, 419.

88 R. L. Quirino, T. F. Garrison and M. R. Kessler, *Green Chem.*, 2014, **16**, 1700.

89 P. N. Ciesielski, M. G. Resch, B. Hewetson, J. P. Killgore, A. Curtin, N. Anderson, A. N. Chiaramonti, D. C. Hurley, A. Sanders, M. E. Himmel, C. Chapple, N. Mosier and B. S. Donohoe, *Green Chem.*, 2014, **16**, 2627.

90 A. K. Mohanty, M. Misra and G. Hinrichsen, *Macromol. Mater. Eng.*, 2000, **276-277**, 1–24.

91 S. Sinha Ray and M. Bousmina, *Prog. Mater. Sci.*, 2005, **50**, 962–1079.

92 M. Darder, P. Aranda and E. Ruiz-Hitzky, *Adv. Mater.*, 2007, **19**, 1309–1319.

93 E. Ruiz-Hitzky, M. Darder and P. Aranda, in *Bio-inorganic Hybrid Nanomaterials*, Wiley-VCH Verlag GmbH & Co. KGaA, 2007, pp. 1–40.

94 E. Medeiros, A. Dufresne and W. Orts, in *Starches*, CRC Press, 2009, pp. 205–251.

95 A. Gandini, *Green Chem.*, 2011, **13**, 1061.

96 A. Valdés, A. C. Mellinas, M. Ramos, M. C. Garrigós and A. Jiménez, *Front. Chem.*, 2014, **2**, 6.

97 H.-B. Yue, Y.-D. Cui, P. S. Shuttleworth and J. H. Clark, *Green Chem.*, 2012, **14**, 2009.

98 S. Yang, S. A. Madbouly, J. A. Schrader, G. Srinivasan, D. Grewell, K. G. McCabe, M. R. Kessler and W. R. Graves, *Green Chem.*, 2014, **17**, 380–393.

99 A. Rouilly and L. Rigal, *J. Macromol. Sci. Part C Polym. Rev.*, 2002, **42**, 441–479.

100 L. Lynd, C. Wyman and T. Gerngross, *Biotechnol. Prog.*, 1999, **15**, 777–793.

101 T. A. Hassan, V. K. Rangari and S. Jeelani, *ACS Sustain. Chem. Eng.*, 2014, **2**, 706–717.

102 A. Sorrentino, G. Gorrasi and V. Vittoria, *Environmental Silicate Nano-Biocomposites*, Springer London, London, 2012, vol. 50.

103 V. Rives, *Layered Double Hydroxides: Present and Future*, Nova Publishers, 2001.

104 U. Costantino, F. Marmottini, M. Nocchetti and R. Vivani, *Eur. J. Inorg. Chem.*, 1998, **1998**, 1439–1446.

105 S.-E. Zhu, F. Li and G.-W. Wang, *Chem. Soc. Rev.*, 2013, **42**, 7535–70.

106 G. Gorrasi and A. Sorrentino, *Polym. Degrad. Stab.*, 2013, **98**, 963–971.

107 G. Gorrasi, C. Milone, E. Piperopoulos, M. Lanza and A. Sorrentino, *Appl. Clay Sci.*, 2013, **71**, 49–54.

108 S. J. Eichhorn, *Soft Matter*, 2011, **7**, 303.

109 N. Reddy and Y. Yang, *Green Chem.*, 2005, **7**, 190.

110 T. Kleine, J. Buendia and C. Bolm, *Green Chem.*, 2013, **15**, 160.

111 M. Oliviero, L. Verdolotti, I. Nedi, F. Docimo, E. Di Maio and S. Iannace, *J. Cell. Plast.*, 2012, **48**, 516–525.

112 T. Q. Hu, Ed., *Chemical Modification, Properties, and Usage of Lignin*, Springer US, Boston, MA, 2002.

113 T. Saito, R. H. Brown, M. A. Hunt, D. L. Pickel, J. M. Pickel, J. M. Messman, F. S. Baker, M. Keller and A. K. Naskar, *Green Chem.*, 2012, **14**, 3295.

114 J. Li, G. Gellerstedt and K. Toven, *Bioresour. Technol.*, 2009, **100**, 2556–61.

115 Y. Lvov and E. Abdullayev, *Prog. Polym. Sci.*, 2013, **38**, 1690–1719.

116 M. Liu, Z. Jia, D. Jia and C. Zhou, *Prog. Polym. Sci.*, 2014, **39**, 1498–1525.

117 A. Sorrentino, in *Woodhead Publishing Series in Metals and Surface Engineering*, eds. A. S. H. Makhlouf and I. B. T.-N. and U.-T. F. Tiginyanu, Woodhead Publishing, 2011, pp. 203–234.

118 C. Aimé and T. Coradin, *J. Polym. Sci. Part B Polym. Phys.*, 2012, **50**, 669–680.

119 S. Pavlidou and C. D. Papaspyrides, *Prog. Polym. Sci.*, 2008, **33**, 1119–1198.

120 R. Zhao, P. Torley and P. J. Halley, *J. Mater. Sci.*, 2008, **43**, 3058–3071.

121 L. Verdolotti, M. Lavorgna, M. Oliviero, A. Sorrentino, V. Iozzino, G. Buonocore and S. Iannace, *ACS Sustain. Chem. Eng.*, 2014, **2**, 254–263.

122 G. Landi, F. Fedi, A. Sorrentino, H. C. Neitzert and S. Iannace, 2014, pp. 202–205.

123 T. Mekonnen, P. Mussone, H. Khalil and D. Bressler, *J. Mater. Chem. A*, 2013, **1**, 13379.

124 H. S. Nalwa, *Polymeric nanostructures and their applications*, American scientific publishers, 2007.

125 I. Armentano, M. Dottori, E. Fortunati, S. Mattioli and J. M. Kenny, *Polym. Degrad. Stab.*, 2010, **95**, 2126–2146.

126 B. A. Rozenberg and R. Tenne, *Prog. Polym. Sci.*, 2008, **33**, 40–112.

127 D. Avnir, T. Coradin, O. Lev and J. Livage, *J. Mater. Chem.*, 2006, **16**, 1013.

128 T. Coradin and J. Livage, *Acc. Chem. Res.*, 2007, **40**, 819–26.

129 I. Gill and A. Ballesteros, *Trends Biotechnol.*, 2000, **18**, 282–96.

130 E. Buerlein, Ed., *Handbook of Biomineralization*, Wiley-VCH Verlag GmbH, Weinheim, Germany, 2007.

131 T. M. Harrell, B. Hosticka, M. E. Power, L. Cemke, R. Hull and P. M. Norris, *J. Sol-Gel Sci. Technol.*, 2004, **31**, 349–352.

132 S. Hartmann, D. Brandhuber and N. Hüsing, *Acc. Chem. Res.*, 2007, **40**, 885–94.

133 J. F. Jenck, F. Agterberg and M. J. Droescher, *Green Chem.*, 2004, **6**, 544.

134 M. Hedayati, M. Salehi, R. Bagheri, M. Panjepour and A. Maghzian, *Powder Technol.*, 2011, **207**, 296–303.

135 H. Wu, W. Zhao, H. Hu and G. Chen, *J. Mater. Chem.*, 2011, **21**, 8626.

136 J. B. Sui, D. Xiang, P. Mou and G. H. Duan, *Adv. Mater. Res.*, 2011, **239-242**, 2503–2510.

137 Z. W. Wu, Z. F. Liu and J. Zhao, *Appl. Mech. Mater.*, 2011, **130-134**, 1708–1711.

138 L. Rajput and R. Banerjee, *Cryst. Growth Des.*, 2014, **14**, 2729–2732.

139 T. Ohura, Y. Tsutaki and M. Sakaguchi, *ScientificWorldJournal.*, 2014, **2014**, 127506.

140 B. Ranu and A. Stolle, Eds., *Ball Milling Towards Green Synthesis*, Royal Society of Chemistry, Cambridge, 2014.

141 Y. Liao, Q. Liu, T. Wang, J. Long, Q. Zhang, L. Ma, Y. Liu and Y. Li, *Energy & Fuels*, 2014, **28**, 5778–5784.

142 V. Bugatti, L. Esposito, L. Franzetti, L. Tammaro and V. Vittoria, *Appl. Clay Sci.*, 2013, **75-76**, 46–51.

143 L. Tammaro, U. Costantino, A. Bolognese, G. Sammartino, G. Marenzi, A. Calignano, S. Tetè, F. Mastrangelo, L. Califano and V. Vittoria, *Int. J. Antimicrob. Agents*, 2007, **29**, 417–23.

144 V. Romeo, G. Gorrasi, V. Vittoria and I. S. Chronakis, *Biomacromolecules*, 2007, **8**, 3147–52.

145 R. Pucciariello, C. Bonini, M. D'Auria, V. Villani, G. Giammarino and G. Gorrasi, *J. Appl. Polym. Sci.*, 2008, **109**, 309–313.

146 R. Pucciariello, M. D'Auria, V. Villani, G. Giammarino, G. Gorrasi and G. Shulga, *J. Polym. Environ.*, 2010, **18**, 326–334.

147 U. Costantino, V. Bugatti, G. Gorrasi, F. Montanari, M. Nocchetti, L. Tammaro and V. Vittoria, *ACS Appl. Mater. Interfaces*, 2009, **1**, 668–77.

148 V. Bugatti, U. Costantino, G. Gorrasi, M. Nocchetti, L. Tammaro and V. Vittoria, *Eur. Polym. J.*, 2010, **46**, 418–427.

149 V. Bugatti, G. Gorrasi, F. Montanari, M. Nocchetti, L. Tammaro and V. Vittoria, *Appl. Clay Sci.*, 2011, **52**, 34–40.

150 L. Vertuccio, G. Gorrasi, A. Sorrentino and V. Vittoria, *Carbohydr. Polym.*, 2009, **75**, 172–179.

151 M. Cocca, R. Avolio, G. Gentile, E. Di Pace, M. E. Errico and M. Avella, *Carbohydr. Polym.*, 2015, **118**, 170–82.

152 S. Santangelo, G. Gorrasi, R. Di Lieto, S. De Pasquale, G. Patimo, E. Piperopoulos, M. Lanza, G. Faggio, F. Mauriello, G. Messina and C. Milone, *Appl. Clay Sci.*, 2011, **53**, 188–194.

153 G. Gorrasi, E. Piperopoulos, M. Lanza and C. Milone, *J. Phys. Chem. Solids*, 2013, **74**, 1–6.

154 J.-B. Kim, T. Premkumar, O. Giani, J.-J. Robin, F. Schue and K. E. Geckeler, *Macromol. Rapid Commun.*, 2007, **28**, 767–771.

155 P. Mangiacapra, G. Gorrasi, A. Sorrentino and V. Vittoria, *Carbohydr. Polym.*, 2006, **64**, 516–523.

156 G. Gorrasi, V. Bugatti and V. Vittoria, *Carbohydr. Polym.*, 2012, **89**, 132–137.

157 G. Gorrasi, *Carbohydr. Polym.*, 2015, **In press**.

158 T. A. Hassan, V. K. Rangari, V. Fallon, Y. Farooq, S. Jeelani and M. Science, in *NSTI-Nanotech 2010*, 2010, vol. 3, pp. 278–281.